Electric Power Systems Research, *23* (1992) 123–128

A new technique for location of transmission line faults using single-terminal voltage and current data

Omar A. S. Youssef
College of Telecommunication, Jeddah (Saudi Arabia)

(Received September 4, 1991)

Abstract

This paper presents a new technique for location of transmission line faults using voltage and current measurements from one end of the faulted line. The method differs from past techniques in many respects. The main feature of the new technique is that it considers the influence of the remote-end infeed of the transmission line, the effect of the transmission line capacitance, fault resistance, prefault loading conditions, and the effect of mutual coupling between different phases of the line, and then computes with a microprocessor the distance to the fault point without any approximations. It uses recorded phase voltages and currents at the near end, then the fundamental components of the measured signals are extracted using microprocessor filters. The modal values of the extracted signals are computed then processed to indicate the precise location of the fault.

Introduction

Rapid power system repair and service restoration subsequent to a permanent fault on a transmission line are essential conditions of utility operation. With the advent of microprocessor based recording devices, utilities have shown increased interest in implementing accurate fault location techniques. Consequently, several methods have been introduced and implemented during recent years.

Takagi *et al.* [1], Eriksson *et al.* [2], Cook [3] and Wiszniewski [4] proposed techniques which use fault current distribution factors, and prefault and postfault currents and voltages from one line terminal; impedances of equivalent sources connected to the line terminals are used in the computation. In practice, from time to time the distribution factors are changed. Several approximations have also been introduced during the computation process. Richards and Tan [5] proposed an iterative technique which uses several system parameters for estimating the location of faults. They developed a sequence network approach that treats both the fault location and the fault resistance as unknown quantities. Shunt reactance is not modeled, limiting the application of the algorithm to short lines. Schweitzer [6, 7] performed an iterative calculation of the difference in phase angle between the total fault current and the remote-end feed current contribution. A sequence model of the line and remote-end source is used, but the mutual coupling between sequence component networks is ignored, thereby assuming that the phase impedances are balanced. Jeyasurya and Rahman [8, 9] presented an algorithm which is based on using current and voltage information at both line ends and by solving the sequence network of the equivalent power system the location of the fault can be estimated. Johns *et al.* [10] proposed a technique which is based on modal analysis using voltage and current data available at both ends of the protected line section. Sachdev and Agarwal [11] used local digital impedance and relay current data as well as corresponding data from the remote end to calculate the distance to the fault point. This method gives considerable errors for certain locations and the fault resistance estimates are inaccurate for locations near the midpoint of the line where the fault current contributions from both line terminals are equal. Lawrence and Waser [12] developed an algorithm based on Z-transform techniques using time domain representation of voltage and current signals and the phase network model.

This paper presents an accurate algorithm to estimate the location of a transmission line fault.

0378-7796/92/$5.00

© 1992 — Elsevier Sequoia. All rights reserved

The method uses the fundamental frequency voltages and currents measured at one line terminal and takes into consideration the following factors:

(1) remote-end current infeed;

(2) exact transmission line representation (distributed parameter representation) is considered in the computation to account for capacitive currents;

(3) prefault and postfault line currents and voltages are measured and stored and used for computation;

(4) the contribution of current from relay location side to the total fault current at the fault location, assumed to be equal to an impedance ratio [2], is corrected;

(5) no major approximations are carrried out during computation;

(6) a modal analysis is used, permitting the inclusion of unbalanced system impedances caused by untransposed lines.

Development of the algorithm

The method to compute the distance to a fault point is based on the following equations in modal form [13, 14]:

$$V_F = V_S \cosh(Gl) - Z_S I_S \sinh(Gl)$$

$$I''_{SF} = (V''_S/Z_S)\sinh(Gl) - I''_S \cosh(Gl)$$

where l is the distance to the fault point from the sending end of the line; V_S is the modal voltage at the sending end (postfault value), I_S the modal current at the sending end (postfault value), V_F the modal voltage at the fault point (postfault value), I_F the modal fault current (postfault value), V''_S the superimposed modal voltage at the sending end (modal voltage difference between prefault and postfault), and I''_S the superimposed modal current at the sending end (modal current difference between prefault and postfault), and I''_{SF} the modal fault current feeding the fault from the sending end side; Z_S is the modal surge impedance, and Z the transmission line impedance per unit length; $G = T + \mathrm{j}P$ is the propagation constant.

Referring to Fig. 1, for the postfault condition, the modal voltages and currents can be expressed as

$$V_F = V_S \cosh(Gl) - I_S Z_S \sinh(Gl)$$

and the superimposed components of the modal voltages and currents can be expressed as

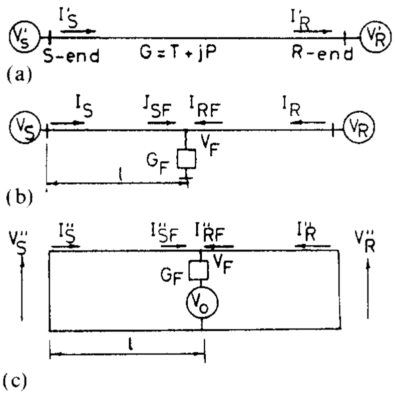

Fig. 1. Single-line diagram of the power system: (a) prefault condition; (b) postfault condition (G_F = fault conductance); (c) superimposed component of fault current.

$$I''_{SF} = (V_S/Z_S)\sinh(Gl) - I''_S \cosh(Gl)$$

In matrix form we can write

$$\boldsymbol{V}_F = [\cosh(Gl)]\boldsymbol{V}_S - [\sinh(Gl)]\boldsymbol{I}_S \qquad (1)$$

$$\boldsymbol{V}_{SF} = [\sinh(Gl)]\mathbf{Y}_S \boldsymbol{V}''_S - [\cosh(Gl)]\boldsymbol{I}''_S \qquad (2)$$

where

$$\boldsymbol{V}_F{}^t = [V_{F1}, V_{F2}, V_{F3}]$$

$$[\cosh(Gl)] = \mathrm{diag}[\cosh(G_1 l), \cosh(G_2 l), \cosh(G_3 l)]$$

$$\boldsymbol{V}_S{}^t = [V_{S1}, V_{S2}, V_{S3}]$$

$$[\sinh(Gl)] = \mathrm{diag}[\sinh(G_1 l), \sinh(G_2 l), \sinh(G_3 l)]$$

$$\mathbf{Z}_S = \mathrm{diag}[Z_{S1}, Z_{S2}, Z_{S3}]$$

$$\mathbf{Y}_S = \mathrm{diag}[Y_{S1}, Y_{S2}, Y_{S3}]$$

$$\boldsymbol{I}''_{SF} = [I''_{SF1}, I''_{SF2}, I''_{SF3}]$$

$$\boldsymbol{I}''_S = [I''_{S1}, I''_{S2}, I''_{S3}]$$

The voltage at the fault location, $\boldsymbol{V}^p_F$, is related to the fault current $\boldsymbol{I}^p_F$ by the fault constraint matrix $\mathbf{G}^p_F$ (where the superscript p indicates phasor values) as follows:

$$\boldsymbol{I}^p_F = \mathbf{G}^p_F \boldsymbol{V}^p_F$$

The fault constraint matrices for different types of faults are indicated in Appendix A, whereas the distribution of the sequence components of currents at the fault location is indicated in Appendix B.

Substituting eqn. (B-1) into eqns. (1) and (2), we get

$$[\sinh(Gl)]\mathbf{Y}_S \boldsymbol{V}''_S - [\cosh(Gl)]\boldsymbol{I}''_S$$
$$= k\mathbf{G}_F\{[\cosh(Gl)]\boldsymbol{V}_S - [\sinh(Gl)]\mathbf{Z}_S\boldsymbol{I}_S\}$$

$$[\cosh(Gl)]\{[\tanh(Gl)]\mathbf{Y}_S \boldsymbol{V}''_S - \mathbf{U}\boldsymbol{I}''_S\}$$
$$= k\mathbf{G}_F[\cosh(Gl)]\{\mathbf{U}\boldsymbol{V}_S - [\tanh(Gl)]\mathbf{Z}_S\boldsymbol{I}_S\}$$
$$k\{\mathbf{U}\boldsymbol{V}_S - [\tanh(Gl)]\mathbf{Z}_S\boldsymbol{I}_S\}$$
$$= [\mathbf{G}_F{}^{-1}]^t\{[\tanh(Gl)]\mathbf{Y}_S \boldsymbol{V}''_S - \mathbf{U}\boldsymbol{I}''_S\}$$

Selecting one of the three modes (e.g. mode 1), and letting

$$\mathbf{F} = [\mathbf{G}_F{}^{-1}]^t$$
$$= \begin{bmatrix} f_{11} & f_{12} & f_{13} \\ f_{21} & f_{22} & f_{23} \\ f_{31} & f_{32} & f_{33} \end{bmatrix}$$

then

$$k[V_{S1} - Z_{S1}\tanh(G_1 l)\, I_{S1}]$$
$$= [f_{11}\, f_{12}\, f_{13}] \begin{bmatrix} \tanh(G_1 l)\ Y_{S1} V''_{S1} - I''_{S1} \\ \tanh(G_2 l)\ Y_{S2} V''_{S2} - I''_{S2} \\ \tanh(G_3 l)\ Y_{S3} V''_{S3} - I''_{S3} \end{bmatrix}$$

$$k[V_{S1} - Z_{S1}\tanh(G_1 l)\, I_{S1}]$$
$$= f_{11}[\tanh(G_1 l)\ Y_{S1} V''_{S1} - I''_{S1}]$$
$$+ f_{12}[\tanh(G_2 l)\ Y_{S2} V''_{S2} - I''_{S2}]$$
$$+ f_{13}[\tanh(G_3 l)\ Y_{S2} V''_{S3} - I''_{S3}] \qquad (3)$$

Equation (3) is a complex equation. It can be split into two separate equations which can be solved to get the two real unknowns k and l. Eliminating k, we get one equation in l, the distance to the fault location from the sending end, in the form

$$f[\tanh(T_1 l), \tan(P_1 l), \tanh(T_2 l),$$
$$\tan(P_2 l), \tanh(T_3 l), \tan(P_3 l)] = 0$$

This equation can be solved by the Newton–Raphson method for successive substitutions, where an initial approximation is assumed for l, that is, l_0, and an iterative process is carried out until the required convergence is achieved. This iterative process is governed by

$$l_{k+1} = l_k - f(l_k)/f'(l_k)$$

The main problem now lies in computing the matrix **F**.

The flowchart of the fault location algorithm is given in Fig. 2.

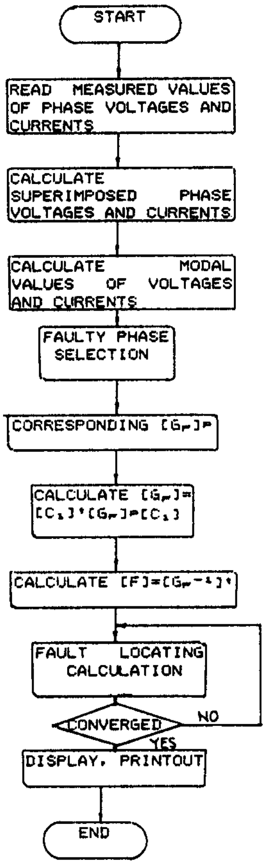
START
READ MEASURED VALUES OF PHASE VOLTAGES AND CURRENTS
CALCULATE SUPERIMPOSED PHASE VOLTAGES AND CURRENTS
CALCULATE MODAL VALUES OF VOLTAGES AND CURRENTS
FAULTY PHASE SELECTION
CORRESPONDING [GF]P
CALCULATE [GF]= [C1]t[GF]P[C1]
CALCULATE [F]=[GF-1]t
FAULT LOCATING CALCULATION
CONVERGED
NO
YES
DISPLAY, PRINTOUT
END

Fig. 2. Flowchart of the fault location algorithm.

TABLE 1. Basic transmission line data

No. of circuits	2
No. of conductors per phase	3
No. of earth wires	2
Conductor position symmetry	None
Conductor resistivity (Ω m)	3.2×10^{-8}
Earth wire resistivity (Ω)	2.69×10^{-8}
Conductor strand diameter (cm)	0.32
Earth wire strand diameter (cm)	0.32
Outer diameter of earth wire (cm)	2.86
No. of effective strands in phase conductor	54
No. of effective strands in earth wire	54
Earth resistivity (Ω m)	20

Test results

The sample power system selected for the studies is a 500 kV, 236 km line section. The basic transmission line data are given in Table 1. Two equivalent power systems were connected to buses R and S. Three types of fault were considered (phase to ground, phase to phase, and double phase to ground). Faults were applied at different locations on the line under different operating conditions. The voltage and current phasors were calculated by the program, then the equivalent modal values were computed. Mode 2 was used in the study. These data were used by

TABLE 2. Results of the study

Fault type	Assumed fault location (p.u.)	Calculated fault location (p.u.)	System condition
Phase to earth	0.6	0.6	Unloaded
Phase to phase	0.6	0.6	$R_F = 50\ \Omega$
Double phase to earth	0.6	0.6006	
Phase to phase	0.7	0.7	Light loading
Phase to phase	0.7	0.7	$R_F = 10\ \Omega$
Double phase to earth	0.7	0.7005	Power flow S to R
Phase to earth	0.9	0.9	Light loading
Phase to phase	0.9	0.9	$R_F = 20\ \Omega$
Double phase to earth	0.9	0.8999	Power flow R to S
Phase to earth	0.2	0.2	Heavy loading
Phase to phase	0.2	0.2	$R_f = \Omega$
Double phase to earth	0.2	0.1998	Power flow S to R

the fault locating algorithm to evaluate the distance to the fault from the sending end. Table 2 summarizes the results of this study.

Conclusion

This paper has presented an accurate algorithm for locating transmission line faults. The algorithm has been tested for a variety of simulated fault conditions, including double-circuit mutual coupling effects, various remote source equivalent conditions, various prefault steady-state conditions, and in the presence of appreciable fault resistance. These simulation studies indicate that the proposed method is accurate for all types of shunt fault at different locations under different operating conditions. The maximum error was found to be 0.1%.

Appendix A

Fault constraint matrices

Referring to Fig. A-1, the fault constraint matrix $\mathbf{G}_F^p$ is given by

(a) for a line to ground fault

$$\mathbf{G}_F^p = y_g \begin{bmatrix} 1 & 0 & 0 \\ 0 & 0 & 0 \\ 0 & 0 & 0 \end{bmatrix}$$

(b) for a line to line fault

$$\mathbf{G}_F^p = \frac{y_F}{2} \begin{bmatrix} 0 & 0 & 0 \\ 0 & 0 & -1 \\ 0 & -1 & 1 \end{bmatrix}$$

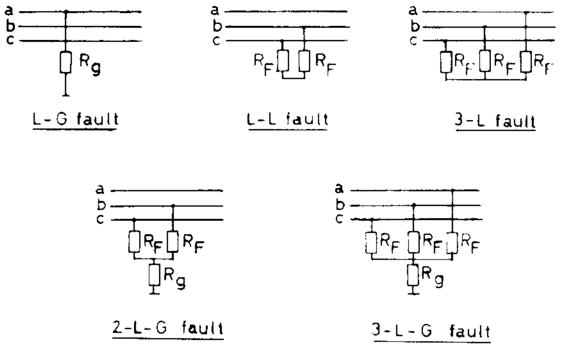

Fig. A-1. Types of fault. R_g is the arc resistance from phase to tower plus the effective tower footing resistance for a single line to ground fault, and the effective tower footing resistance for other types of ground fault. R_F is the arc resistance between faulted phases.

(c) for a three-phase fault

$$\mathbf{G}_F^p = \frac{y_F}{3} \begin{bmatrix} 2 & -1 & -1 \\ -1 & 2 & -1 \\ -1 & -1 & 2 \end{bmatrix}$$

(d) for a double line to ground fault

$$\mathbf{G}_F^p = \frac{1}{R_F^2 + 2R_F R_g} \begin{bmatrix} 0 & 0 & 0 \\ 0 & R_F + R_g & -R_g \\ 0 & -R_g & R_F + R_g \end{bmatrix}$$

(e) for a three-phase to ground fault

$$\mathbf{G}_F^p = \frac{1}{3} \begin{bmatrix} y_0 + 2y_F & y_0 - y_F & y_0 - y_F \\ y_0 - y_F & y_0 + 2y_F & y_0 - y_F \\ y_0 - y_F & y_0 - y_F & y_0 + 2y_F \end{bmatrix}$$

where

$$y_0 = 1/(R_F + 3R_g)$$

The phase quantities $\boldsymbol{V}^p$ and $\boldsymbol{I}^p$ are related to the modal quantities $\boldsymbol{V}$ and $\boldsymbol{I}$ by the eigenvector matrices $\mathbf{C}_1$ and $\mathbf{C}_2$:

$$\boldsymbol{V}^p = \mathbf{C}_1 \boldsymbol{V}$$

$$\boldsymbol{I}^p = \mathbf{C}_2 \boldsymbol{I}$$

Since we have

$$\boldsymbol{I}_F^p = S_1 \mathbf{G}_F^p \boldsymbol{V}_F^p$$

where S_1 is a real quantity representing the fault resistance,

$$S_1 = \begin{cases} y_g & \text{for a line to ground fault} \\ y_F/2 & \text{for a line to line fault} \\ y_F/3 & \text{for a three-phase fault} \end{cases}$$

For a double line to ground fault,

$$S_1 = 1/(R_F{}^2 + 2R_F{}^2 R_g)$$

$$\mathbf{G}_F^p = R_F \begin{bmatrix} 0 & 0 & 0 \\ 0 & 1 & 0 \\ 0 & 0 & 1 \end{bmatrix} + R_g \begin{bmatrix} 0 & 0 & 0 \\ 0 & 1 & -1 \\ 0 & -1 & 1 \end{bmatrix}$$

In this paper R_g is taken to be equal to R_F.

For a three-phase to ground fault,

$$S_1 = y_F$$

$$\mathbf{G}_F^p = \frac{y_0 - y_F}{3y_F} \begin{bmatrix} 1 & 1 & 1 \\ 1 & 1 & 1 \\ 1 & 1 & 1 \end{bmatrix} + \begin{bmatrix} 1 & 0 & 0 \\ 0 & 1 & 0 \\ 0 & 0 & 1 \end{bmatrix}$$

Appendix B

Distribution of sequence components of currents at fault location

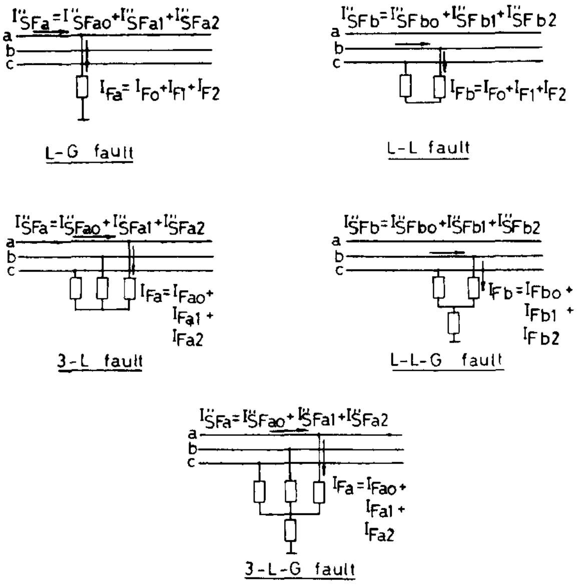

Fig. B-1. Distribution of sequence components of currents at the fault location.

Referring to Fig. B-1, the phase relation between the fault current I_F and the fault current from the sending end is governed by the current distribution factors k_0, k_1, and k_2 of the sequence components:

$$k_0 = I''_{SF0}/I_{F0}$$

$$k_1 = I''_{SF1}/I_{F1}$$

$$k_2 = I''_{SF2}/I_{F2}$$

We can assume to a high degree of accuracy that $k_1 = k_2$, so that

$$\begin{aligned} I''_{SF}/I_F &= (I''_{SF0} + I''_{SF1} + I''_{SF2})/(I_{F0} + I_{F1} + I_{F2}) \\ &= [k_0 I_{F0} + k_1(I_{F1} + I_{F2})]/I_F \\ &= k_1 + (k_0 - k_1)I_{F0}/I_F \end{aligned}$$

(a) For a single line to ground fault,

$$I_F = 3I_{F0}$$

and

$$I''_{SFa}/I_F = k_1 + (k_0 - k_1)/3 = k_{LG}$$

(b) For a line to line fault,

$$I_{F0} = 0$$

$$I''_{SFb}/I_{Fb} = k_1 = k_{LL}$$

(c) For a three-phase fault,

$$I_{F0} = 0$$

and

$$I''_{SFa}/I_{Fa} = k_1 = k_{3L}$$

(d) For double line to ground and three-phase to ground faults,

$$I''_{SFa}/I_{Fa} = k_1 + (k_0 - k_1)I_{F0a}/I_{Fa}$$

$$I''_{SFb}/I_{Fb} = k_1 + (k_0 - k_1)I_{F0b}/I_{Fb}$$

$$I''_{SFc}/I_{Fc} = k_1 + (k_0 - k_1)I_{F0c}/I_{Fc}$$

But

$$I_{F0a} = I_{F0b} = I_{F0c} = I_{F0}$$

and

$$I''_{\mathrm{SF0a}} = I''_{\mathrm{SF0b}} = I''_{\mathrm{SF0c}} = k_0 I_{\mathrm{F0}}$$

Let

$$(k_0 - k_1) I''_{\mathrm{SF0}} / k_0 = C_0$$

then

$$\begin{bmatrix} I''_{\mathrm{SFa}} - C_0 \\ I''_{\mathrm{SFb}} - C_0 \\ I''_{\mathrm{SFc}} - C_0 \end{bmatrix} = k_1 \begin{bmatrix} I_{\mathrm{Fa}} \\ I_{\mathrm{Fb}} \\ I_{\mathrm{Fc}} \end{bmatrix}$$

or

$$\begin{bmatrix} I''_{\mathrm{SFa}} \\ I''_{\mathrm{SFb}} \\ I''_{\mathrm{SFc}} \end{bmatrix} = k_1 \begin{bmatrix} I_{\mathrm{Fa}} \\ I_{\mathrm{Fb}} \\ I_{\mathrm{Fc}} \end{bmatrix} + C_0 \begin{bmatrix} 1 \\ 1 \\ 1 \end{bmatrix}$$

In the case of double line to ground and three-phase line to ground faults, k_1 is assumed to be equal to k_0, that is, $C_0 = 0$.

Hence, $\boldsymbol{I}''^{\mathrm{p}}_{\mathrm{SF}}$ can be represented by a real fraction, k_{F}, of the total fault current $\boldsymbol{I}^{\mathrm{p}}_{\mathrm{F}}$ (e.g. k_{LG}, k_{LL}, k_{3L}, k_{2LG}, k_{3LG}), that is, the angle of the fault current $\boldsymbol{I}_{\mathrm{F}}$ and the fault current from the sending end, $\boldsymbol{I}''_{\mathrm{SF}}$, are assumed to be equal.

In phasor form

$$\boldsymbol{I}''^{\mathrm{p}}_{\mathrm{SF}} = k_{\mathrm{F}} \boldsymbol{I}^{\mathrm{p}}_{\mathrm{F}}$$

$$\boldsymbol{I}''^{\mathrm{p}}_{\mathrm{SF}} = S_1 k_{\mathrm{F}} \mathbf{G}^{\mathrm{p}}_{\mathrm{F}} \boldsymbol{V}^{\mathrm{p}}_{\mathrm{F}}$$

In modal form

$$\begin{aligned} \boldsymbol{I}''_{\mathrm{SF}} &= S_1 k_{\mathrm{F}} \mathbf{C}_2{}^{-1} \mathbf{G}^{\mathrm{p}}_{\mathrm{F}} \mathbf{C}_1 \boldsymbol{V}_{\mathrm{F}} \\ &= k \mathbf{G}_{\mathrm{F}} \boldsymbol{V}_{\mathrm{F}} \end{aligned} \tag{B-1}$$

where

$$\begin{aligned} \mathbf{G}_{\mathrm{F}} &= \mathbf{C}_2{}^{-1} \mathbf{G}^{\mathrm{p}}_{\mathrm{F}} \mathbf{C}_1 \\ &= \mathbf{C}_1{}^{\mathrm{t}} \mathbf{G}^{\mathrm{p}}_{\mathrm{F}} \mathbf{C}_1 \end{aligned}$$

References

1 T. Takagi *et al.*, Development of a new type fault locator using one terminal voltage and current data, *IEEE Trans., PAS-101* (1982) 2892–2898.

2 L. Eriksson, *et al.*, An accurate fault locator with compensation for apparent reactance in the fault resistance resulting from remote-end infeed, *IEEE Trans., PAS-104* (1985) 424–436.

3 V. Cook, Fundamental aspect of fault location algorithm used in distance protection, *Proc. Inst. Electr. Eng., Part C, 133* (1986) 359–368.

4 A. Wiszniewski, Accurate fault impedance locating algorithm, *Proc. Inst. Electr. Eng., Part C, 130* (1983) 311–314.

5 G. C. Richards and O. T. Tan, An accurate fault location estimation for transmission lines, *IEEE Trans., PAS-101* (1982) 945–950.

6 E. Schweitzer and J. Jachinowski, A prototype microprocessor-based system for transmission line protection and monitoring, *8th Annu. Western Protective Relay Conf., Spokane, WA, USA 1981.*

7 E. Schweitzer, Evaluation and development of transmission line fault-locating techniques which use sinuosidal steady-state information, *9th Annu. Western Protective Relay Conf., Spokane, WA, USA, 1982.*

8 B. Jeyasurya and M. A. Rahman, Accurate fault location of transmission lines using microprocessors, *IEE Conf. Publ. No. 249*, (1989) 13–17.

9 B. Jeyasurya and M. A. Rahman, A comparative study of transmission line fault locating algorithm, *Proc. Nat. Conf. Microprocessor Applications in Power Systems, Nagpur, India, 1988*, pp. 131–146.

10 A. T. Johns, S. Jamali and S. M. Hadan, New accurate transmission line fault location equipment, *IEE Conf. Publ. No. 249*, (1989) 1–5.

11 M. S. Sachdev and R. K. Agarwal, Accurate fault-location estimates from digital impedance relay measurements, *IEE Conf. Publ. No. 249*, (1989) 180–184.

12 D. J. Lawrence and D. L. Waser, Transmission line fault location using digital fault recorders, *IEEE Trans., PWRD-3* (2) (1988) 496–502.

13 L. M. Wedepohl, Application of matrix methods to the solution of travelling-wave phenomena in polyphase systems, *Proc. Inst. Electr. Eng., 110* (1963) 2200–2212.

14 R. H. Galloway and L. M. Wedepohl, Calculation of electrical parameters for short and long polyphase transmission lines, *Proc. Inst. Electr. Eng., 111* (1964) 2051–2059.